

Single-mode GaSb-based laterally coupled distributed-feedback laser for CO_2 gas detection

Shi-Xian Han(韩实现), Jin-Yi Yan(严进一), Chun-Fang Cao(曹春芳), Jin Yang(杨锦), An-Tian Du(杜安天), Yuan-Yu Chen(陈元宇), Ruo-Tao Liu(刘若涛), Hai-Long Wang(王海龙), and Qian Gong(龚谦)
Citation: Chin. Phys. B, 2023, 32 (**10**): 104205. DOI: 10.1088/1674-1056/accff2
Journal homepage: http://cpb.iphy.ac.cn; http://iopscience.iop.org/cpb

What follows is a list of articles you may be interested in

Mode characteristics of VCSELs with different shape and size oxidation apertures

Xin-Yu Xie(谢新宇), Jian Li(李健), Xiao-Lang Qiu(邱小浪), Yong-Li Wang(王永丽), Chuan-Chuan Li(李川川), and Xin Wei(韦欣)
Chin. Phys. B, 2023, 32 (**4**): 044206. DOI: 10.1088/1674-1056/ac9821

Single-mode lasing in a coupled twin circular-side-octagon microcavity

Ke Yang(杨珂), Yue-De Yang(杨跃德), Jin-Long Xiao(肖金龙), and Yong-Zhen Huang(黄永箴)
Chin. Phys. B, 2022, 31 (**9**): 094205. DOI: 10.1088/1674-1056/ac6802

Numerical study of converting beat-note signals of dual-frequency lasers to optical frequency combs by optical injection locking of semiconductor lasers

Chenhao Liu(刘晨浩), Haoshu Jin(靳昊澍), Hui Liu(刘辉), and Jintao Bai(白晋涛)
Chin. Phys. B, 2022, 31 (**8**): 084205. DOI: 10.1088/1674-1056/ac649a

Multi-target ranging using an optical reservoir computing approach in the laterally coupled semiconductor lasers with self-feedback

Dong-Zhou Zhong(钟东洲), Zhe Xu(徐喆), Ya-Lan Hu(胡亚兰), Ke-Ke Zhao(赵可可), Jin-Bo Zhang(张金波),Peng Hou(侯鹏), Wan-An Deng(邓万安), and Jiang-Tao Xi(习江涛)
Chin. Phys. B, 2022, 31 (**7**): 074205. DOI: 10.1088/1674-1056/ac4021

All-fiber erbium-doped dissipative soliton laser with multimode interference based on saturable-reserve saturable hybrid optical switch

Xin Zhao(赵鑫), Renyan Wan(王仁严), Weiyan Li(李卫岩), Liang Jin(金亮), He Zhang(张贺), Yan Li(李岩), Yingtian Xu(徐英添), Linlin Shi(石琳琳), and Xiaohui Ma(马晓辉)
Chin. Phys. B, 2022, 31 (**6**): 064215. DOI: 10.1088/1674-1056/ac5611

Single-mode GaSb-based laterally coupled distributed-feedback laser for CO_2 gas detection

Shi-Xian Han(韩实现)[1,2], Jin-Yi Yan(严进一)[1], Chun-Fang Cao(曹春芳)[1], Jin Yang(杨锦)[1], An-Tian Du(杜安天)[1,3], Yuan-Yu Chen(陈元宇)[1], Ruo-Tao Liu(刘若涛)[1,2], Hai-Long Wang(王海龙)[3], and Qian Gong(龚谦)[1,†]

[1] *Key Laboratory of Terahertz Solid State Technology, Shanghai Institute of Microsystem and Information Technology, Shanghai* 200050, *China*
[2] *Center of Materials Science and Optoelectronics Engineering, University of Chinese Academy of Sciences, Beijing* 100049, *China*
[3] *Shandong Provincial Key Laboratory of Laser Polarization and Information Technology, School of Physics and Physical Engineering, Qufu Normal University, Qufu* 273165, *China*

(Received 23 March 2023; revised manuscript received 24 April 2023; accepted manuscript online 25 April 2023)

We report on a GaSb-based laterally coupled distributed feedback (LC-DFB) laser with Cr gratings operating at 2004 nm for CO_2 detection application. Butterfly packaged with single-mode fiber pigtailed, the laser diode operates in the continuous-wave mode in a temperature range from −10 °C to 60 °C, with a maximum output power of 2 mW and a maximum side-mode suppression ratio over 30 dB. Wavelength-modulated absorption spectroscopy of CO_2 demonstrates the applicability of the LC-DFB laser to tunable diode laser absorption spectroscopy. Furthermore, the diode junction temperature, which is measured by using the wavelength shift method, exhibits a maximum value of 17 °C in the single-mode operation range.

Keywords: semiconductor lasers, quantum wells, laser spectroscopy

PACS: 42.55.Px, 78.67.De, 42.62.Fi **DOI:** 10.1088/1674-1056/accff2

1. Introduction

Gas detection based on tunable laser diode absorption spectroscopy (TDLAS) is based on scanning the wavelength of a narrow linewidth laser across the rotational-vibrational absorption line of a specific gas molecule and analyzing the absorption spectrum.[1] The development of the TDLAS technology has been stimulated by the high standards required for industrial process control,[2] medicine and pollution detection,[3] and high sensitivity detection requirements.[4] In a typical TDLAS system, custom-made diode laser operating at a particular wavelength aiming at a specific gas absorption line is indispensable as a key light source component. For example, a laser wavelength of about 2 μm is significant in detecting CO_2 gas due to its strong characteristic absorption.[5] Although Fabry–Perot (FP) edge-emitting GaSb laser diodes have been used in trace-gas spectroscopy, their applications are largely restricted by multimode operation and undesirable random mode hopping behaviors. It is, thus, important to develop continuous-wave (CW) distributed-feedback (DFB) lasers that are workable in single mode and tunable near 2 μm for the targeted CO_2 gas absorption lines.

In this work, GaSb-based LC-DFB lasers with Cr gratings are fabricated, without the regrowth process used in traditional DFB laser fabrication.[6] The LC-DFB laser is designed to operate at 2004 nm for CO_2 detection with the first-order gratings. The butterfly packaged LC-DFB laser with 4-μm-wide ridge operates under CW mode with a threshold current of 19 mA. The side mode suppression ratio (SMSR) is larger than 30 dB over the tuning wavelength region of 2.4 nm. Furthermore, the applicability of the proposed laser to detecting CO_2 gas is also proved by a simplified TDLAS system based on wavelength-modulated absorption spectroscopy. Finally, the maximum junction temperature is estimated at 17 °C by measuring the shift in the emission wavelength that occurs due to temperature.

2. Fabrication

The laser structure was grown on an n-type GaSb (100) substrate using molecular beam epitaxy equipment. The grown structure started with a 100-nm-thick Te-doped (1×10^{18} cm^{-3}) GaSb buffer. The $Al_{0.9}GaAsSb$ n-type cladding layer was comprised of an 857-nm-thick layer and a 979-nm-thick layer, which had been Te-doped at 2×10^{18} cm^{-3} and 5×10^{17} cm^{-3}, respectively, in order to reduce the absorption of free carriers.[7] Two 12-nm-thick InGaSb quantum wells separated with a 25-nm-thick $Al_{0.25}GaAsSb$ barrier were centered at a 356-nm-thick undoped $Al_{0.25}GaAsSb$ waveguide core layer. Then, Be doped p-type cladding layer with the same thickness as the n-type cladding layer was grown. Finally, the growth was completed by a 100-nm-thick Be-doped (1×10^{19} cm^{-3}) GaSb layer as a contact layer.

After growth, LC-DFB lasers were fabricated with Cr gratings. The cross-sectional view of the laser ridge and top

†Corresponding author. E-mail: qgong@mail.sim.ac.cn

© 2023 Chinese Physical Society and IOP Publishing Ltd

view of the Cr gratings obtained by scanning electron microscopy are shown in Fig. 1. The 4-μm-wide ridge was fabricated via dry etching by using the gases of Ar, Cl_2, and BCl_3. First-order Cr gratings were exposed alongside the ridge by using electron beam lithography (EBL), and followed by the deposition of Cr layer by electron beam evaporation, as well as the lift-off process. The grating period was 288.8 nm designed by using the Bragg formula for a target Bragg wavelength of 2004 nm. Subsequently, a 200-nm-thick SiN_x layer was deposited as a passivation layer. For p- and n-contacts, Ti/Pt/Au layer and GeAu/Ni/Au layer were evaporated, respectively. Finally, the chip was cleaved into bars each with a dimension of 0.4 mm×0.5 mm and was packaged in a 14-pin butterfly package with a single-mode optical fiber.

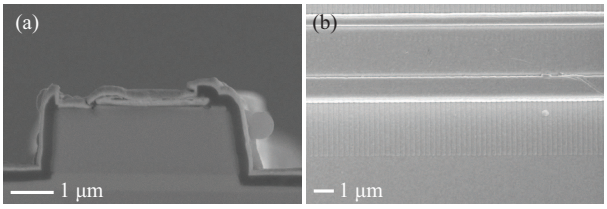


Fig. 1. (a) Cross-sectional view of LC-DFB laser. (b) Top view of Cr gratings covered by SiN_x and electrode thin film.

3. Results

3.1. Electro-optical characterization

The LC-DFB laser is tested under the CW operation mode, and the current–voltage–power characteristics of this laser are shown in Fig. 2(a). The device shows a threshold current of 19 mA at 20 °C, corresponding to a threshold current density of 950 A/cm^{-2}, which is roughly 1.15 times higher than that of the FP lasers fabricated from the same structure. This minor increase in the threshold current is likely to be caused by the small optical loss, owing to the Cr gratings. As shown in Fig. 2(a), the device operates in the single mode at temperature ranging from −10 °C to 60 °C. The forward voltage rises with the decrease of operating temperature, resulting from the combined effect of intrinsic carrier concentration, band-gap energy, and effective density.[8] Figure 2(b) shows the lasing spectra recorded at −5 °C with injection current varying, measured by a grating type optical spectrum analyzer (Yokogawa AQ6376) with a resolution of 0.1 nm, which limits the measured line width to gigahertz level. Therefore, the line width of the LC-DFB laser is measured by a scanning Fabry–Perot interferometer (Thorlabs SA201-12B) with a better resolution of 67 MHz. The laser line width is obtained to be 85.5 MHz, which is around the measurement limit of our interferometer. The stable single-mode operation generates emissions of wavelengths ranging from 2002.36 nm to 2004.76 nm, with the SMSR values over 30 dB for all the tests. The current tuning speed (0.10 nm/mA) is slightly higher than that of a typical DFB laser,[9] which implies that a lower amplitude of tuning current is sufficient to cover the CO_2 gas absorption wavelength (i.e. 2004 nm) required for TDLAS applications. The output optical power from the fiber is more than 1.5 mW when the laser operates at the wavelength of 2004 nm.

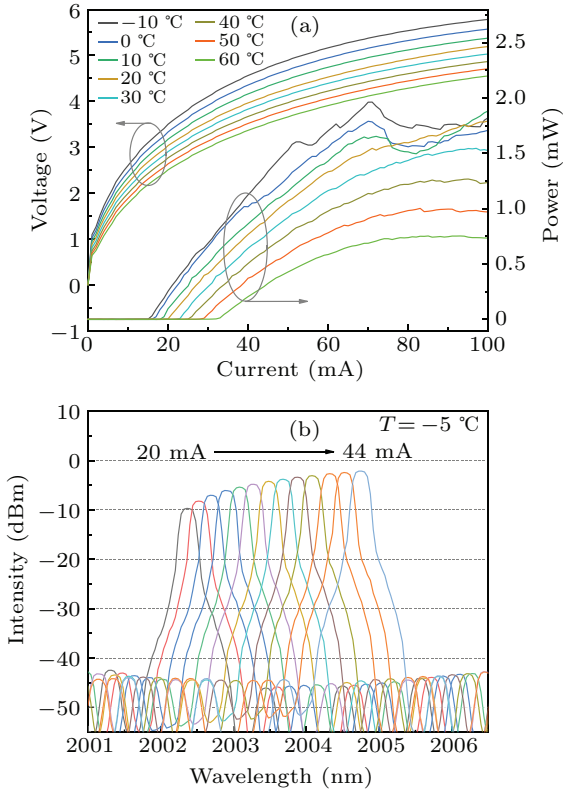


Fig. 2. (a) Current–voltage–power characteristics of LC-DFB laser at temperatures ranging from −10 °C to 60 °C. (b) Emission spectra observed at injection currents ranging from 20 mA to 44 mA and −5 °C near the target CO_2 absorption wavelength of 2004 nm.

3.2. Gas measurements

In order to further verify the application of this laser to the CO_2 gas detection, a simplified experimental TDLAS platform is set up by using the principle of wavelength-modulated absorption spectroscopy as shown in Fig. 3(a). The system involves the wavelength length modulation, gas absorption, and data processing. The wavelength modulation is implemented by driving the LC-DFB laser with a signal generator (Rigol DG1032Z), a temperature controller (Thorlabs ITC4020), and a current controller (Thorlabs LDC210A). Based on the HITRAN database for CO_2 gas absorption near 2.0 μm as shown in Fig. 3(b), the central frequency of the CO_2 gas absorption line is chosen as 4990.0 cm^{-1} (2004 nm) to avoid the absorption peaks of the H_2O gas. As shown in the inset of Fig. 3(b), the full width at half maximum (FWHM) of the selected gas absorption line is 0.064 nm. A composite signal consisting of a symmetrical sawtooth signal and a sinusoidal signal is generated to drive the laser through the current controller. To ensure that the laser operates at a specific wavelength, the diode temperature is maintained at −8.5 °C. Thus, the laser wavelength is slowly scanned through the absorption line at a

speed of 0.10 nm/mA by using a 10-Hz sawtooth wave with (41 mA±3 mA)-injection currents. At the same time, the laser wavelength is modulated by a 5-kHz sinusoidal wave with an amplitude of ±2.4 mA, which corresponds to a wavelength modulation factor (ratio of the modulation amplitude to the gas linewidth) of 2.2.[1] Then, the gas absorption is completed by coupling the light into a 75-cm-long gas cell filled with CO_2 in wet N_2 (water vapor concentration of 0.07%) under 1 atm (1 atm = 1.01325×10^5 Pa) and 298 K. An InGaAs detector with extended cutoff wavelength is used to collect the light transmitted through the CO_2 gas and generate signals carrying gas absorption information, which is displayed on an oscilloscope (Rigol, DS2072A). The recorded signals are shown in Fig. 4(a). An obvious depression (highlighted by the blue circles) is observed in the spectra owing to the CO_2 gas absorption. Naturally, the spectrum corresponding to the high CO_2 concentration of 4% has a stronger absorption signal than that in the low concentration case (0.03%) as shown in Fig. 4(a). Moreover, the 2f harmonic signal spectra are extracted by a lock-in amplifier (EG & G 7265) and shown in Fig. 4(b). The correlation of the absorption signal mentioned above is well verified by the 2f harmonic signal spectra.

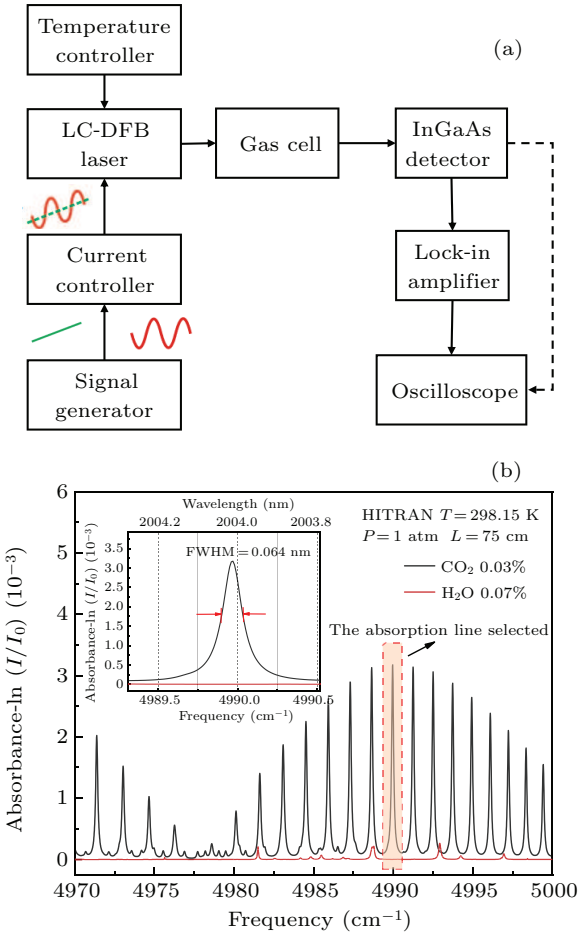


Fig. 3. (a) Flowchart depicting TDLAS system. (b) Absorption spectrum of 0.03% CO_2 and 0.07% water vapor at 1 atm, 298 K, and an absorption length of 75 cm, with inset showing magnified part of absorption line with FWHM of 0.064 nm (from HITRAN database).

Therefore, the application of the LC-DFB laser to the CO_2 gas detection is verified in this work. However, the signal-to-noise ratio is somewhat low, which might be affected by system factors such as detector shot noise, detector thermal noise, laser linewidth, optical feedback to the laser due to scattering from components,[10] etc.

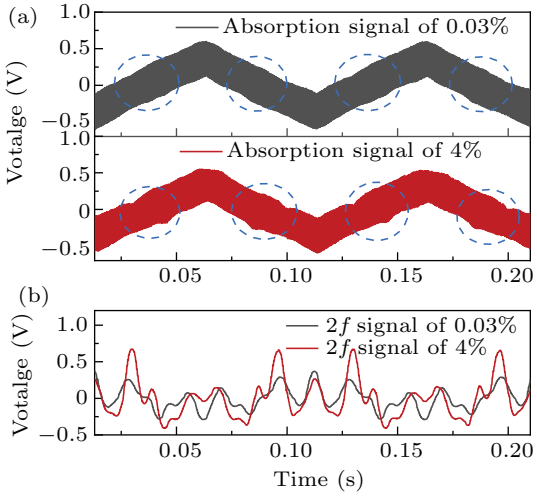


Fig. 4. Measured waveforms of (a) absorption signal and (b) 2f harmonic signal at CO_2 concentrations of 0.03% and 4%.

3.3. Temperature characteristics

Since the applications of TDLAS rely heavily on the wavelength tunability of laser source and, at the same time, the lasing wavelength is temperature-dependent, the temperature characteristics of the LC-DFB laser is studied below. The dominant factor of wavelength tuning in a laser diode is the change of effective refractive index of the material in the laser structure, owing to the thermal effect of injection current. Usually, the junction temperature in the CW mode may be significantly higher than the ambient temperature.[11] In addition, the thermal effect may also affect other device performance characteristics such as internal efficiency, maximum output power, stability, and lifetime. Various methods of measuring the junction temperatures of different kinds of light emitting diodes have been proposed, such as AlGaInP/GaAs LEDs, InAs/InP(100) quantum-dot lasers, GaN-based laser diodes, etc., including the extraction of the junction temperature from external parameters, e.g. voltage,[12,13] power,[14] and wavelength.[14,15] Here, the junction temperature is measured by using the wavelength shift method, which involves pulse-wave (PW) measurement and CW measurement. For the PW measurement, the LC-DFB laser is driven by a square-shaped pulse current (with a pulse width of 200 ns, a pulse period of 200 μs, corresponding to a duty cycle of 0.1%) to ensure that heating effect can be ignored. Therefore, junction temperature (T_J) can be assumed to be equal to the operation temperature (T_{op}). The PW measurement also establishes the relationship between the emission wavelength and T_J, which

can be expressed as follows:

$$\Delta\lambda_{\rm p} = K_\lambda \cdot \Delta T_{\rm op}, \tag{1}$$

where K_λ is the temperature coefficient of wavelength at $T_{\rm op}$, and $\lambda_{\rm p}$ is the wavelength lasing under pulsed current conditions. In CW measurement, the PW result is used to deduce $T_{\rm J}$ under the CW mode by using the following equations:

$$\Delta T_{\rm J} = (\lambda_{\rm c} - \lambda_{\rm p})/K_\lambda, \tag{2}$$

$$T_{\rm J} = T_{\rm op} + \Delta T_{\rm J}, \tag{3}$$

where $\lambda_{\rm c}$ is the wavelength under CW current condition, $T_{\rm J}$ is the junction temperature in CW mode, and $\Delta T_{\rm J}$ is the increment of junction temperature due to heating effect.

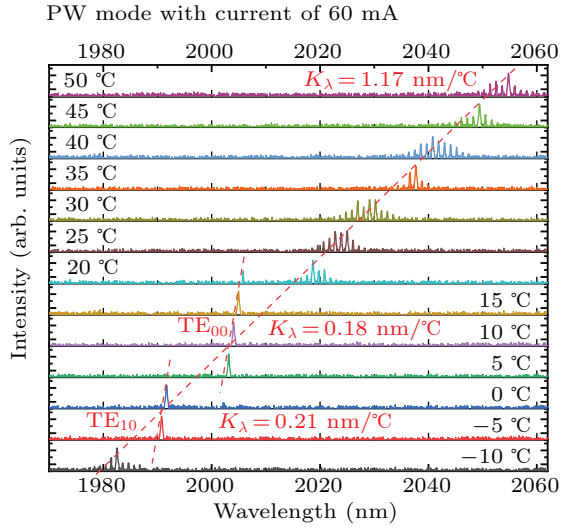


Fig. 5. Evolutions of emission intensity with wavelength at injection current of 60 mA, different wavelengths, and operation temperatures ranging from −10 °C to 60 °C.

The variation in spectrum intensity with $T_{\rm op}$ is illustrated in Fig. 5. The measurements are performed at a fixed injection current of 60 mA in a temperature range of −10 °C to 50 °C. Two single-mode operating ranges are observed. The fundamental mode TE_{00} emits the target Bragg wavelength in a temperature range of 5 °C–15 °C, which evolves from 2002 nm to 2005.8 nm. The wavelength of the shorter single mode TE_{10} varies from 1991 nm to 1993 nm. The difference in wavelength between the TE_{00} mode and the TE_{10} mode is approximately 11 nm, which corresponds to the difference in refractive index between the TE_{00} (3.469) mode and the TE_{10} modes (3.4502). Meanwhile, the TE_{00} mode exhibits K_λ value of 0.18 nm/°C and the TE_{10} mode exhibits K_λ value of 0.21 nm/°C. The gain profile is red-shifted with temperature rising at a rate of 1.17 nm/°C, which is much higher than that observed with DFB modes. Mode hop and multimode occur owing to the overlap and mismatch between the gain curve and the DFB modes with increasing operating temperature, which should be avoided when LC-DFB laser is utilized in TDLAS. Figure 6 shows that the variation in DFB emission wavelength with injection current is measured from −9 °C to 5 °C, where the laser operates in the TE_{00} mode. The calculated $T_{\rm J}$ value is displayed on the right coordinate. The TE_{00} mode dominates when $T_{\rm J}$ is in a range from −1 °C to 17 °C. For junction temperatures outside of the range mentioned above, the TE_{10} mode or multi-mode operation mode may dominate. Thick gold plating layer acting as a heat spreader on the top of the contact layer or epi-side down mounting are alternative methods of reducing $T_{\rm J}$. In this way, the operation temperature at which TE_{00} mode dominates can be improved. Finally, the thermal resistance of the device is deduced to be 101 K/W which is similar to the value reported previously.[17]

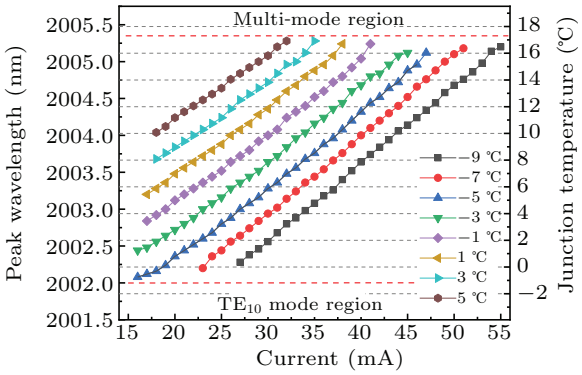


Fig. 6. Evolutions of emission spectra with current at different operation temperatures, an injection current of 60 mA under different peak wavelengths, currents, and junction temperatures.

4. Conclusions

In summary, we demonstrated an LC-DFB GaSb-based quantum well laser with butterfly packaging and fiber output, operating at 2004 nm. The first-order Cr gratings are fabricated alongside the ridge by using EBL. The pigtailed laser diode operated in the CW mode with maximum output power as high as 2 mW. The wavelength of the single longitudinal mode shifts from 2002.36 nm to 2004.76 nm when the injection current increases from 20 mA to 44 mA, at a rate of 0.10 nm/mA. A single absorption line at 2004 nm of the CO_2 gas is chosen and the measured absorption spectrum clearly proves that the LC-DFB laser can be used in the TDLAS . Finally, it is found that the device operates in the TE_{00} mode when the junction temperature is in a range of −1 °C to 17 °C, characterized by the wavelength shift method.

Acknowledgement

Project supported by the Shanghai Municipal Science and Technology Major Project, China (Grant No. 2017SHZDZX03).

References

[1] Hodgkinson J and Tatam R P 2013 *Meas. Sci. Technol.* **24** 012004
[2] Lackner M 2007 *Reviews in Chemical Engineering* **23** 65
[3] Sauer C G, Pisano J T and Fitz D R 2003 *California Atmospheric Environment* **37** 1583

[4] Jia J, Li W, Chai ao, Zhang S, Zhang M, Cui H, Liu J and Liu Z 2019 *Infrared and Laser Engineering* **48** 517007

[5] Yang C, Xie S, Zhang Y, Shang J, Huang S S, Yuan Y, Shao F, Zhang Y, Xu Y and Niu Z 2019 *Appl. Phys. Lett.* **114** 021102

[6] Miller L M, Verdeyen J T, Coleman J J, Bryan R P, Alwan J J, Beernink K J, Hughes J S and Cockerill T M 1991 *IEEE Photon. Technol. Lett.* **3** 6

[7] Xu L, Forrest S R, Menna R, Martinelli R and Connolly J C 1996 *Electron. Lett.* **32** 1717

[8] Xi Y, Xi J Q, Gessmann Th, Shah J M, Kim J K, Schubert E F, Fischer A J, Crawford M H, Bogart K H A and Allerman A 2005 *Appl. Phys. Lett.* **86** 031907

[9] Yang C A, Xie S W, Huang S S, Yuan Y, Zhang Y, Shang J M, Zhang Y, Xu Y Q and Niu Z C 2019 *IEEE Photon. Technol. Lett.* **31** 210

[10] Wall K 2006 *A Review of Tunable Diode Laser Absorption Spectroscopy* (Toronto)

[11] Schiff H I, Mackay G I and Bechara J 1994 *Res. Chem. Intermed.* **20** 525

[12] Li J Y, Du Z H, Ma Y W and Xu K X 2013 *Chin. Phys. B* **22** 034203

[13] Asmari A, Hodgkinson J, Chehura E, Staines S E and Tatam R P 2014 *SPIE Photonics Europe* (Brussels, Belgium) p. 91351A

[14] Asmari A, Hodgkinson J, Chehura E, Staines S E and Tatam R P 2017 *Opt. Express* **25** 11679

[15] Kim D S, Holloway C, Han B and Bar-Cohen A 2016 *Appl. Opt.* **55** 7487

[16] Cheng W H, Wang S C, Yang Y D, Chi S, Sheen M T and Kuang J H 1997 *IEEE Trans. Comp., Packag., Manufact. Technol. B* **20** 396

[17] Zhu C, Zhang Y G, Li A Z and Zheng Y L 2005 *Semicond. Sci. Technol.* **20** 563